Collision-Induced Transitions within the Levels of 4p Configuration of Ar II

By

Kunihide TACHIBANA* and Kuniya FUKUDA*

(Received September 30, 1972)

Abstract

On the basis of a semi-empirical calculation of plasma parameters, the change of the population density induced by the laser field modulation at 4880 Å ($4p^2D^0_{5/2}-4s^2P^0_{3/2}$) has been observed as a function of atom or electron density for the laser upper level and a third level, any one in the 4p configuration of Ar II. In this situation the anisotropic intensity distribution of spontaneous radiation around the laser tube axis is analyzed so as to relate the change of the radiation to that of the population density for the transitions of interest. Further, by the use of a rate equation developed for the modulated population density of the third level, the rate coefficient is derived for the transition between this and the laser upper levels from the observed changes of population densities of these levels. The values of the rate coefficients for the collisional transitions are obtained for all levels of the 4p cofiguration, and in connection with this result the configuration temperature of this configuration is discussed.

1. Introduction

The modulation of the laser field changes the population densities not only of the laser upper and lower levels but also of a third level connected with them through collisional or radiative process. This phenomenon has been observed by many investigators[1~15] in gas laser experiments. From the analysis of this phenomenon the rate coefficients for the transitions by atomic or electronic collision can be deduced when the changes of the population densities are observed on many third levels as a function of atom or electron density. For NeI in a He-Ne laser, for example, Parks and Javan[2] obtained the rate coefficients for the transitions by atomic collision within the levels of 4s configuration, and Khaikin[5,9] determined those between the levels belonging to different configurations, *e. g.*, 4p′ and 4d′. For an ion laser, however, there are only a few experiments of laser field modulation,[12,14,16] and the

* Department of Mechanical Engineering II.

determination of the rate coefficients has never been carried out. The main reason for this is a lack in information of plasma parameters, *e. g.*, atom or electron density and temperature, for a systematic experiment to be made on the laser.

In a previous paper,[17] the calculation of plasma parameters in an Ar ion laser was presented, which is in good agreement with the measured ones. In the present paper, on the basis of the calculated plasma parameters, the rate coefficients for the transitons within the levels of the 4p configuration of Ar II will be determined for atomic and electronic collisions separately.

In the next section, the rate equation for the modulated population density of the third level will be developed. Section 3 will desiribe how to obtain the population density change from the observed intensity change of spontaneous emission for the level of interest, where the analysis is given for the anisotropic distribution of the emission around the laser tube axis caused by the polarization of laser field. In the last section, the obtained collisional rate coefficients are listed and compared with the radiative decay rates. Further, the so-called "configuration temperature" of the 4p configuration will be discussed in connection with this result.

2. Rate Equation

In the following, the laser upper and lower levels are denoted by 2 and 1, respectively, and any third level by 3, which is connected with the laser upper level through an atomic or an electronic collision process. When the laser field is modulated, the population density of level 2 is changed and at the same time that of level 3 is also changed. If the modulation of the laser field is sufficiently slower than the characteristic times of collisional and radiative processes in a positive column, the population densities are in respective steady states at the presence and at the absence of the laser field. When transitions by multiple collision processes are neglected and only direct transitions are considered, the rate equation for the third level can be written as follows : at the presence of the laser field

$$\frac{dn_3}{dt} = R_3 + (Q_{23}^a n_0 + Q_{23}^e n_e) n_2 - (W_3 + \sum_i Q_{3i}^a n_0 + \sum_j Q_{3j}^e n_e) n_3 = 0 \tag{1.1}$$

and at the absence of the field

$$\frac{dn_3'}{dt} = R_3' + (Q_{23}^a n_0' + Q_{23}^e n_e') n_2' - (W_3 + \sum_i Q_{3i}^a n_0' + \sum_j Q_{3j}^e n_e') n_3' = 0, \tag{1.2}$$

where n_0 and n_e are the atom and charged particle (ion or electron) densities, n_2 and n_3 the population densities of levels 2 and 3, respectively, R_3 the excitation rate to level 3 from all levels other than the level 2, W_3 the radiative decay rate

from level 3, and Q^a_{ij} and Q^e_{ij} the transition rate coefficient from level i to j due to the collisions with atoms and charged particles, respectively. If it is assumed that $R_3=R_3'$, $n_0=n_0'$ and $n_e=n_e'$ hold, Eqs. (1.1) and (1.2) are reduced to

$$(Q^a_{23}n_0+Q^e_{23}n_e)\Delta n_2=(W_3+\sum_i Q^a_{3i}n_0+\sum_j Q^e_{3j}n_e)\Delta n_3, \tag{2}$$

where $\Delta n_i=n_i-n_i'$.

When it is assumed that the transition rates by charged particle collision as well as by atom collision are small in comparison with W_3 in the right hand side of the above equation, Eq. (2) becomes

$$\frac{\Delta n_3}{\Delta n_2}=\frac{Q^e_{23}}{W_3}n_e+\frac{Q^a_{23}}{W_3}n_0. \tag{3}$$

Therefore, if n_0 is kept at a constant value, one can obtain Q^e_{23} from the gradient of the straight line of $\Delta n_3/\Delta n_2$ with the known W_3.

Next, when it is assumed that n_e depends linearly on n_0, *i. e.*, $n_e=kn_0$,*

$$\frac{\Delta n_2}{\Delta n_3}=\frac{W_3}{Q^a_{23}+kQ^e_{23}}\frac{1}{n_0}+\frac{\sum_i Q^a_{3i}+k\sum_j Q^e_{3j}}{Q^a_{23}+kQ^e_{23}}. \tag{4}$$

Therefore, plotting $\Delta n_2/\Delta n_3$ against $1/n_0$, one can obtain Q^a_{23} from the gradient of the straight line with the known W_3 and the Q^e_{23} obtained beforehand. In the above procedures, it is assumed that the dependence of the cross section on the kinetic temperature of particles is small for the transitions by the collisions with atoms and charged particles. This assumption is, of course, allowed in the experimental ranges of plasma parameters.

3. Experiment

The experimental setup is shown schematically in Fig. 1. The dimensions of the capillaries of the laser tube and test cell were 2.0 and 2.5 mm in bore radius and 45 and 7 cm in length, respectively. Both tubes were placed in a cavity, which is composed of a concave reflecting mirror and a Littrow prism, and discharges were excited by respective sources. Discharge current I and filling gas pressure p_0 of the laser tube were fixed at 7 A and 0.5 Torr, respectively. On the other hand, those

* This assumption is allowed in the narrow range of n_0, *i. e.*, the gas pressure in an ion laser tube. In a wider range of n_0, n_e is approximately proportional to $n_0^{1/2}$.[17]

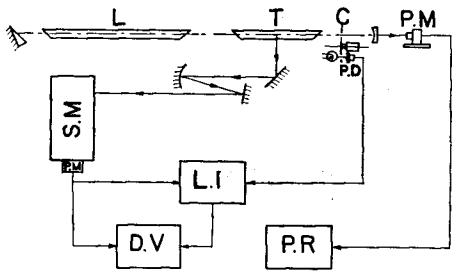

Fig. 1. Schematic diagram of the experimental setup. L : laser tube, T : test cell, C : rotating chopper, P. M : photomultiplier, S. M : spectrometer, L. I : lock-in amplifier, D. V. : digital voltmeter and P. R : pen recorder.

of the test cell were varied in the range of 1~7 A and 0.1~1.0 Torr.

Laser oscillation was tuned at 4880 Å ($4p^2D^o_{5/2}-4s^2P^o_{3/2}$) and the laser field was modulated at a frequency of 4 kHz by a rotating chopper. In general, the discharge current and voltage are affected by the modulation of the laser field,[10] but in the present experimental setup the effect on the test cell is considered to be negligibly small because of its shorter length and larger bore radius.[2,5,9] Further, the present setup enabled us to select the discharge current and filling gas pressure of the test cell in a wide range with very little change of the laser field.

The changes of spontaneous emissions from levels 2 and 3 (ΔI_2 and ΔI_3) were observed in the direction of the electric field of laser light. The image of the central part of the positive column (100 μm in width and 2 cm in length) was focused onto the entrance slit of a 1 m Ebert type spectrometer. Then the output signal of a EMI photomultiplier was fed into a lock-in amplifier, the reference signal for which was produced by a lamp and a photodiode put on the opposite sides of the chopper. The calibration of the optical system including the spectrometer and the photomultiplier was performed with a standard lamp of NBS EPUV-1143.

The observed ΔI_2 is not only polarized[8] but also distributed anisotropically around the tube axis because of the polarization of the laser field in the cavity.[6] But it is not polarized in the direction of the electric field of the laser field (position A in Fig. A-1 of Appendix), which is proved by the detailed calculation in the Appendix following the method of Dunn and Maitland.[8] The ratio of the observed ΔI_2 from 4082 and 4228 Å transitions with the same upper level is about 2,* which is in good agreement with the value without magnetic field in position A of Table A-3

* The relative intensities of spontaneous emissions from both the lines were also measured and the observed ratio of the transition probabilities was found to be within 10% agreement with the ratio of the tabulated values (W. L. Wiese, M. W. Smith, and B. Miles : *Atomic Transition Probabilities*, Vol. II, NSRDS-NBS 22 (1969)).

in Appendix. Therefore, it is concluded that, in the test cell, the self-induced magnetic field by its own discharge current is weak enough to be neglected.

The modulated population density of level 2 is given by Eq. (A.2) and Table A-1 of Appendix ;

$$\Delta n_2 = \frac{\sum_M \Delta n\ (\alpha, M)}{g_2} = const. \times \frac{1}{3g_2} S^{\alpha}_{\alpha''} |\boldsymbol{E}|^2, \tag{5}$$

where g_2 is the statistical weight of level 2. On the other hand the observed ΔI_2 in the case of no magnetic field is represented by Eq. (A. 8) or (A. 9) for the transition $\Delta J=1$ or $\Delta J=0$, respectively. Therefore, Δn_2 is given by

$$\Delta n_2 = const. \frac{\Delta I_2}{3g_2(\nu^{\alpha}_{\alpha''})^4(96/3600)S^{\alpha}_{\alpha''}} = const. \frac{1.667\ \Delta I_2}{\nu^{\alpha}_{\alpha''} g_2 A^{\alpha}_{\alpha''}} \tag{6}$$

for $\Delta J = 1$ and

$$\Delta n_2 = const. \frac{\Delta I_2}{3g_2(\nu^{\alpha}_{\alpha''})^4(616/12600)S^{\alpha}_{\alpha''}} = const. \frac{0.909\ \Delta I_2}{\nu^{\alpha}_{\alpha''} g_2 A^{\alpha}_{\alpha''}} \tag{7}$$

for $\Delta J=0$, where the relation $A^{\alpha''}_{\alpha}$=const. $\times(\nu^{\alpha}_{\alpha''})^3 S^{\alpha}_{\alpha''}/g_2$ has been used. The observation was carried out on the 4228 Å ($\Delta J=1$) and 4082 Å ($\Delta J=0$) transitions and Δn_2 was determined as the average value of Eqs. (6) and (7) for both the transitions.

On the contrary, ΔI_3 is isotropic around the tube axis since polarization is destroyed on the third level through collisonal transitions. Therefore, substituting Δn_3 for $\Delta n(\alpha, M)$ in Eq. (A.6), one obtains

$$\begin{aligned} \Delta I_3 &= const. \times (\nu^{\alpha}_{\alpha''})^4\ \Delta n_3 \sum_M \sum_{M''} [S^{\alpha}_{\alpha'' M''}\ f(\theta, \Delta M, \boldsymbol{a})] \\ &= const. \times (\nu^{\alpha}_{\alpha''})^4\ \Delta n_3 \frac{2}{3} S^{\alpha}_{\alpha''}. \end{aligned} \tag{8}$$

Then Δn_3 becomes

$$\Delta n_3 = const. \times \frac{\frac{3}{2}\Delta I_3}{\nu^{\alpha}_{\alpha''} g_3 A^{\alpha}_{\alpha''}}. \tag{9}$$

The intensity change ΔI_3 was observed on many emission lines from the levels of 4p configuration so as to derive the population density change Δn_3 from Eq. (9).

The relative intensities of spontaneous emissions from the levels of the 4p configuration were also measured without the modulation of the laser field to give the population density distribution within the configuration. The configuration

temperature of the 4p configuration can be derived from the Boltzmann plot of these population densites.

4. Results and Discussions

The population densities of the laser lower level as well as the upper level are changed by the modulation of the laser field. However, the life of the former is extremely shorter than that of the latter, and the ratio of the modulated population desities, $\Delta n_1/\Delta n_2$, is less than 1/100 for an argon ion laser.[20] Moreover, in the present experimental setup, the changes of discharge parameters due to the modulation are small enough to keep the conditions of $R_3=R_3'$, $n_0=n_0'$ and $n_e=n_e'$. Therefore, the population density change of a level 3 of the 4p configuration is attributed to the transition from level 2.

Tables 1 and 2 are the measured valuse of $\Delta n_3/\Delta n_2$ for all levels of the 4p configuration in two cases, *i. e.*, one in which n_e is varied under a constant n_0, and

Table 1. Modulated populatin densities of 4p levels relative to that of $^2D^o_{5/2}$ at various disiharge currents.

	$\Delta n_3 / \Delta n_2$					
p_0 (Torr)	0.276	0.305	0.343	0.586	0.633	0.826
I (A)	1.3	1.6	2.0	3.0	5.0	7.0
n_0 (10^{16}cm^{-3})	0.483	0.483	0.438	0.483	0.483	0.483
n_e (10^{13}cm^{-3})	1.06	1.22	1.66	2.50	4.25	6.08
$^4P^o_{5/2}$	0.034	0.039	0.053	0.106	0.065	0.073
$^4P^o_{3/2}$	0.031	0.057	0.031	0.063	0.045	0.058
$^4P^o_{1/2}$	0.033	0.041	0.052	0.055	0.094	0.145
$^4D^o_{7/2}$	0.012	0.037	——	0.047	0.039	0.068
$^4D^o_{5/2}$	0.021	0.060	0.041	0.051	0.068	0.106
$^4D^o_{3/2}$	0.015	0.015	——	0.045	0.127	0.063
$^4D^o_{1/2}$	0.014	0.042	0.022	0.013	0.035	0.066
$^2D^o_{5/2}$	1.000	1.000	1.000	1.000	1.000	1.000
$^2D^o_{3/2}$	0.078	0.068	0.081	0.063	0.045	0.058
$^2P^o_{1/2}$	0.057	0.028	0.065	0.066	0.055	0.062
$^2P^o_{3/2}$	0.021	0.020	0.041	0.029	0.025	0.048
$^4S^o_{3/2}$	0.026	0.038	0.020	0.023	0.055	0.068
$^2S^o_{1/2}$	0.024	0.033	0.017	0.042	0.036	0.072

Table 2. Modulated population densities of 4p levels relative to that of $^2D^o_{5/2}$ at various pressurers.

	$\Delta n_3 / \Delta n_2$							
p_0 (Torr)	0.1	0.13	0.16	0.2	0.3	0.5	0.7	1.0
I (A)	3.0	3.0	3.0	3.0	3.0	3.0	3.0	3.0
n_0 (10^{16}cm^{-3})	0.110	0.143	0.176	0.220	0.329	0.449	0.770	1.10
n_e (10^{13}cm^{-3})	1.26	1.41	1.57	1.75	2.11	2.68	3.15	3.69
$^4P^o_{5/2}$	0.021	0.021	0.040	0.023	0.083	0.055	0.055	0.060
$^4P^o_{3/2}$	0.020	0.019	0.025	0.043	0.093	0.049	0.077	0.082
$^4P^o_{1/2}$	0.027	0.033	0.021	0.046	0.079	0.102	0.058	0.093
$^4D^o_{7/2}$	0.015	0.014	0.017	0.020	0.029	0.022	0.033	0.035
$^4D^o_{5/2}$	0.027	0.021	0.029	0.044	0.070	0.082	0.052	——
$^4D^o_{3/2}$	0.025	0.043	0.030	0.047	0.061	0.081	0.137	0.124
$^4D^o_{1/2}$	0.008	0.009	0.011	0.020	0.035	0.066	0.043	0.084
$^2D^o_{5/2}$	1.000	1.000	1.000	1.000	1.000	1.000	1.000	1.000
$^2D^o_{3/2}$	0.016	0.016	0.019	0.029	0.038	0.047	0.043	0.074
$^2P^o_{1/2}$	0.020	0.018	0.016	0.019	0.033	0.049	0.040	0.078
$^2P^o_{3/2}$	0.012	0.008	0.011	0.020	0.033	0.040	0.020	0.105
$^4S^o_{3/2}$	0.007	0.011	0.004	0.012	0.024	0.015	0.026	0.043
$^2S^o_{1/2}$	0.006	0.009	0.011	0.026	0.034	0.047	0.038	0.039

the other in which n_0 is varied under a constant discharge current, respectively. The values of n_0 and n_e are the net atom density under the gas drive-out effect[19] and the charged particle density (electron or ion) calculated by the method of ref. 17, respectively. In order to obtain the values of Q^e_{23} and Q^a_{23}, the data in Tables 1 and 2 are plotted according to Eqs. (3) and (4), where $k = 4.35 \times 10^{-3}$ has been used.[17] Figures 2 and 3 show some examples of the plots, and the obtained values of the rate coefficients are listed in Table 3.

The effect of multiple collisions has been neglected in the above treatment. In order to verify this assumption, a calculation for a simplified model is done as follows. When this effect is taken into consideration, the following equation must be used for level i in stead of Eq. (2);

$$\sum_j [Q^a_{ji} n_0 + Q^e_{ji} n_e] \Delta n_j - [W_i + \sum_k Q^a_{ik} n_0 + \sum_l Q^e_{il} n_e] \Delta n_i = 0. \qquad (10)$$

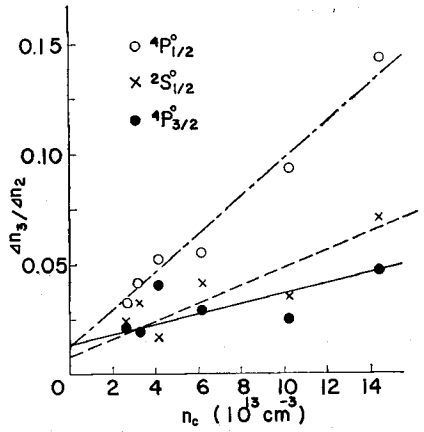

Fig. 2. The plots of $\Delta n_3/\Delta n_2$ for some levels as a function of n_e.

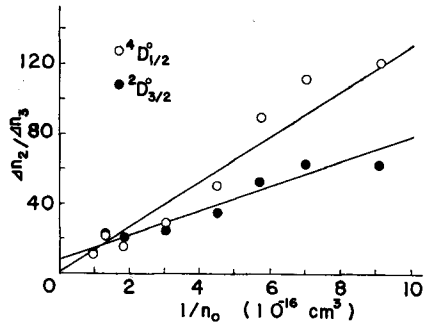

Fig. 3. The plots of $\Delta n_2/\Delta n_3$ for some levels as a function of $1/n_0$.

Table 3. Transition rate coefficients from $^2D^o_{5/2}$ by collisions of charged particles and neutral atoms.

	Q^e_{2j}	Q^a_{2j}
j	10^{-7}cm^3 / sec	10^{-9}cm^3 / sec
$^4P^o_{5/2}$	2.0	3.3
$^4P^o_{3/2}$	1.1	2.4
$^4P^o_{1/2}$	4.6	2.2
$^4D^o_{7/2}$	2.3	2.0
$^4D^o_{5/2}$	2.1	2.2
$^4D^o_{3/2}$	2.2	3.2
$^4D^o_{1/2}$	1.9	0.5
$^2D^o_{3/2}$	0	2.0
$^2P^o_{1/2}$	0	1.3
$^2P^o_{3/2}$	0.6	1.3
$^4S^o_{3/2}$	1.2	2.4
$^4S^o_{1/2}$	1.6	0.9

For simplicity, it is assumed here that collisional transitions by charged particles do not occur but only transitions between adjacent levels by atomic collision are present. Further, by referring to the values of Table 3, the transition rates are represented by one value of $Q^a_{i,i+1}=2\times10^{-9}$ cm^3 sec^{-1} for any i and the backward transition is

expressed by

$$Q^{a}_{i+1,i} = Q^{a}_{i,i+1} \exp[(E_{i+1} - E_i)/kT_a] \tag{11}$$

from the assumption of a detailed balance, where the atom temperature T_a is given by the empirical formula of Chester.[19] A set of 13 rate equations for all the levels i of the 4p configuration are solved simultaneously by a computer. The obtained Δn_i for all but $^2D^o_{3/2}$ and $^4D^o_{1/2}$ levels adjecent to the laser upper level $^2D^o_{5/2}$ indicate the population change due to the multiple collisions. In Fig. 4 the calculated values of $\Delta n_i/\Delta n_2$ for all third levels are compared with the measured ones, which

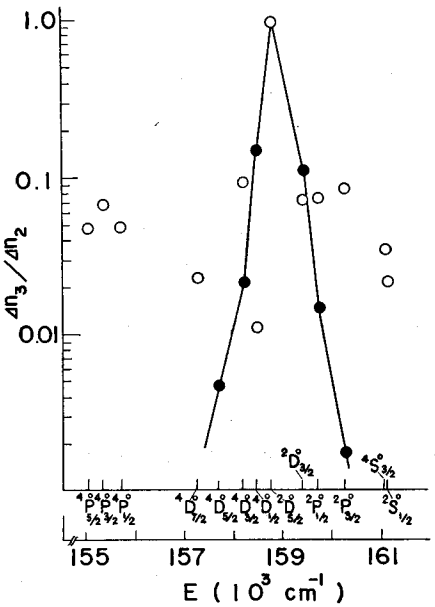

Fig. 4. Comparison between the calculated values of $\Delta n_3/\Delta n_2$ (•) and the measured ones (○) for all 4p levels at $p_0=1.0$ Torr and $I=3$ A.

are corrected for the contribution from charged particle collisions. The effect of multiple collisions is about 20% for the $^4D^o_{3/2}$ and $^2P^o_{1/2}$ levels and becomes much smaller for other levels far from them. The result of Fig. 4 corresponds to the case of a rather high filling gas pressure and the effect becomes smaller for lower gas pressure. From the above result, it is concluded that the effect of multiple collisions can be neglected in the present experiment.

From the values of Table 3, the rate for a transition between the 4p sublevels of Ar II by atomic collison, $n_0 Q^a_{ij}$, is estimated at most 10^7 sec^{-1} ($n_0 \simeq 10^{16}$ cm^{-3}) in its

order of magnitude in the pressure range of the experiment. The transition probability of spontaneous emission from any one of those levels is about 10^8 sec^{-1}. From this fact it is expected that the configuration temperature determined from the population density distribution among the 4p levels does not coincide with the kinetic temperature of atoms. In fact, as shown in Fig. 5, the observed configuration temparature T_c falls far from the atom temparature T_a calculated from the Chester formula.

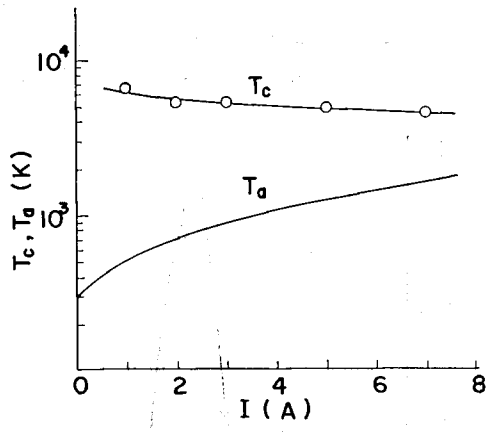

Fig. 5. Observed cofiguration temperature T_c and calculated atom temperature T_a as a function of discharge current.

In this figure the increase in the discharge current (or n_e) makes T_a higher but the configuration temperature remains nearly constant.

Appendix

The polarization and the anisotropy of the modulated spontaneous emission have been described by several authors.[6,8] A theoretical calculation is made here after the method of Dunn and Maitland[8] to apply to the present experiment. However, some corrections are made on their errors.

We assume that the stimulated emission loss from the sublevel (α, M) is given by

$$\Delta n\ (\alpha, M) = const. \times B\ (\alpha, M)\ I, \qquad (A.1)$$

where M denotes the magnetic quantum number and α a set of quantum numbers of the level other than M. Further, $B(\alpha, M)$ is a coefficient describing the stimulated emission process and I the intensity of the laser field. Now, the geometrical arrangement is settled as shown in Fig. A-1, *i. e.*, the magnetic field direction **B**, viewing direction **V** and polarization direction of the laser radiation **E** are all in the same plane and perpendicular to the laser axis. The angle ϕ between **V** and **E** is zero

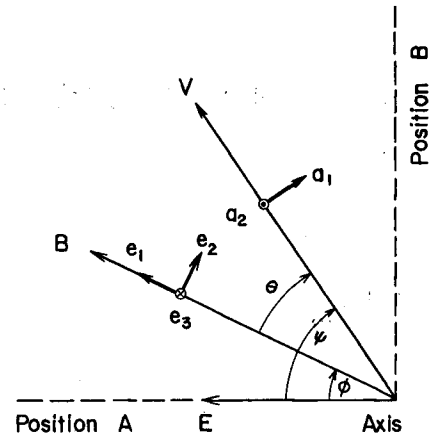

Fig. A-1. Geometrical arrangement

for position A and $\frac{1}{2}\pi$ for position B. Then the laser field can be decomposed of three components, *i. e.*, σ component $|\boldsymbol{E}|\cos\phi\cdot\boldsymbol{e}_1$, which stimulates transitions of $\Delta M=0$, π_+ component $\frac{1}{2}|\boldsymbol{E}|\sin\phi\cdot(\boldsymbol{e}_2+i\boldsymbol{e}_3)$ which does that of $\Delta M=+1$ and π_- component $\frac{1}{2}|\boldsymbol{E}|\sin\phi\cdot(\boldsymbol{e}_2-i\boldsymbol{e}_3)$ which does that of $\Delta M=-1$, where $\boldsymbol{e}_1$, $\boldsymbol{e}_2$ and $\boldsymbol{e}_3$ are unit vectors shown in Fig. A-1. Then Eq. (A.1) becomes

$$\Delta n\,(\alpha, M) = const. \times \left[S^{\alpha M}_{\alpha' M}\cos^2\phi+\frac{1}{2}(S^{\alpha M}_{\alpha' M-1}+S^{\alpha M}_{\alpha' M+1})\sin^2\phi\,|\boldsymbol{E}|^2\right], \tag{A.2}$$

where $S^{\alpha M}_{\alpha' M'}$ is the square of the matrix element for a transition from an upper laser sublevel (α, M) to a lower one (α', M').

The intensity change of a spontaneous emission from the laser sublevel (α, M) to a sublevel (α'', M'') of any lower state is given by

$$\Delta I\,(\alpha M\,;\,\alpha''M''\,;\,\boldsymbol{a}) = const. \times(\nu^{\alpha}_{\alpha''})^4\,\Delta n(\alpha, M)S^{\alpha M}_{\alpha'' M''}f(\theta, M, \boldsymbol{a}), \tag{A.3}$$

where $\nu^{\alpha}_{\alpha''}$ is the frequency of the emission and $f(\theta, M, \boldsymbol{a})$ a geometric factor which depends on θ, M and the direction of polarization $\boldsymbol{a}$. Representing $\boldsymbol{a}$ by $\boldsymbol{a}_1$ and $\boldsymbol{a}_2$ as shown in Fig. A-1, one obtains for $\Delta M=0$

$$f(\theta, 0, \boldsymbol{a}_1) = \sin^2\theta. \qquad f(\theta, 0, \boldsymbol{a}_2) = 0 \tag{A.4}$$

and for $\Delta M = \pm 1$

$$f(\theta, \pm 1, \boldsymbol{a}_1) = \frac{1}{2}\cos^2\theta, \qquad f(\theta, \pm 1, \boldsymbol{a}_2) = \frac{1}{2} \tag{A.5}$$

Therefore, the sum of the intensity changes over all upper and lower sublevels

becomes

$$\Delta I(\alpha, \alpha'', \boldsymbol{a}) = const. \times (\nu_{\alpha''}^{\alpha})^4 \sum_{M} \sum_{M''} [\Delta n(\alpha, M) S_{\alpha'' M''}^{\alpha M} f(\theta, \Delta M, \boldsymbol{a})]. \tag{A.6}$$

In general, $S_{\alpha'' M''}^{\alpha M}$ can be written by the $3J$ symbol and a square of the reduced matrix element $S_{\alpha''}^{\alpha}$ as follows ;[21]

$$S_{\alpha'' M''}^{\alpha M} = \begin{pmatrix} J & 1 & J'' \\ -M & q & M'' \end{pmatrix}^2 S_{\alpha''}^{\alpha}, \tag{A.7}$$

where the numbers in parenthesis denote the $3J$ symbol and $q = M - M''$. Squares of the $3J$ sybolms for the transitions 4228 Å ($4p^2D^o_{5/2} - 4s^4P^o_{3/2}$; $\Delta J = 1$) and 4082 Å ($4p^2D^o_{5/2} - 4s^4P^o_{5/2}$; $\Delta J = 0$) are given in Tables A-1 and A-2, respectively. Therefore Eq. (A.6) becomes

Table A-1. Squares of the $3J$ symbols for the transition $4p^2D^o_{5/2} - 4s^4P^o_{3/2}$.

M for $4s^4P^o_{3/2}$ \ M for $4p^2D^o_{5/2}$	+5/2	+3/2	+1/2	−1/2	−3/2	−5/2
+3/2	10/60	4/60	1/60			
+1/2		6/60	6/60	3/60		
−1/2			3/60	6/60	6/60	
−3/2				1/60	4/60	10/60

Table A-2. Squares of the $3J$ symbols for the transition $4s^4P^o_{5/2} - 4p^2D^o_{5/2}$.

M for $4s^4P^o_{5/2}$ \ M for $4p^2D^o_{5/2}$	+5/2	+3/2	+1/2	−1/2	−3/2	−5/2
+5/2	25/210	10/210				
+3/2	10/210	9/210	16/210			
+1/2		16/210	1/210	18/210		
−1/2			18/210	1/210	16/210	
−3/2				16/210	9/210	10/210
−5/2					10/210	25/210

$$\Delta I\ (4p^2D^o_{5/2}\ ;\ 4s^4P^o_{3/2}\ ;\ \boldsymbol{a}) = const. \times (\nu^a_{a''})^4$$
$$\times \frac{1}{3600}\left[\{(48\sin^2\phi + 104\cos^2\phi)\sin^2\theta + (76\sin^2\phi + 48\cos^2\phi)\cos^2\theta\}\boldsymbol{a}_1\right.$$
$$\left. + (76\sin^2\phi - 48\cos^2\phi)\boldsymbol{a}_2\right] S^a_{a'}, S^a_{a''}|\boldsymbol{E}|^2 \qquad (A.8)$$

for 4228 Å and

$$\Delta I\ (4p^2D^o_{5/2}\ ;\ 4s^4P^o_{3/2}\ ;\ \boldsymbol{a}) = const. \times (\nu^a_{a''})^4$$
$$\times \frac{1}{12600}\left[\{(308\sin^2\phi + 84\cos^2\phi)\sin^2\theta + (196\sin^2\phi + 308\cos^2\phi)\cos^2\theta\}\boldsymbol{a}_1\right.$$
$$\left. + (196\sin^2\phi + 308\cos^2\phi)\boldsymbol{a}_2\right] S^a_{a'}, S^a_{a''}|\boldsymbol{E}|^2 \qquad (A.9)$$

for 4082 Å.

Polarization ratios and modulated intensities of the two spontaneous emissions

Table A-3. Polarzation ratios and relative intensities of modulated emissions of 4228 Å and 4082 Å.

		no field		self-field	
	position	4228Å	4082Å	4228Å	4082Å
polarization ratio (direction)	A	0	0	0.029 ($\boldsymbol{a}_2$)	0.027 ($\boldsymbol{a}_1$)
	B	0.368 ($\boldsymbol{a}_1$)	0.571 ($\boldsymbol{a}_2$)	0.124 ($\boldsymbol{a}_1$)	0.161 ($\boldsymbol{a}_2$)
relative intensity	A	1.600	2.933	2.008	2.467
	B	2.533	1.867	2.358	2.067

are listed in Table A-3 for two cases. In one case a magnetic field is not present ($\phi=0$) ; and in the other, a self-induced magnetic field around the tube axis by its own discharge current is present, where Eqs. (A·8) and (A. 9) must be averaged over ϕ.

References

1) A. L. Waksberg and A. I. Carswell : Appl. Phys. Letters, **6**, 137 (1965).
2) J. H. Parks and A. Javan : Phys. Rev., **139**, A1351 (1965).
3) L. A. Weaver and R. J. Freiberg : J. Appl. Phys., **37**, 1528 (1966).
4) V. M. Kaslin, G. G. Petrash and A. S. Khaikin : Opt. and Spectr., **13**, 14 (1967).
5) A. S. Khaikin : Soviet Phys. -JETP, **24**, 25 (1967).
6) Th. Hänsch and P. Toschek : Phys. Letters, **22**, 150 (1966).
7) R. J. Freiberg and L. A. Weaver : J. Appl. Phys., **38**, 250 (1967).
8) M. H. Dunn and A. Maitland : Proc. Phys. Soc., **92**, 1106 (1967).

9) A. S. Khaikin : Soviet. Phys. -JETP, **27**, 28 (1968).
10) H. Merkelo, R. H. Wright, E. P. Bialecke and J. P. Kaplafka : Appl. Phys. Letters, **12**, 337 (1968).
11) R. A. Lilly and J. R. Holmes : J. Opt. Soc. America, **58**, 1406 (1968).
12) M. H. Dunn : J. IEEE Quant. Electr., **QE-4**, 357 (1968).
13) H. Merkelo, R. H. Wright, J. P. Kaplafka and E. P. Bialecke : Appl. Phys. Letters, **13**, 401 (1968).
14) A. Ferrario, A. Sironi and A. Sona : Appl. Phys. Letters, **14**, 174 (1969).
15) T. Sakurai, T. Ohta and T. Ogawa : Japan. J. Appl. Phys., **10**, 234 (1971).
16) R. I. Rudko and C. I. Tang : J. Appl. Phys., **38**, 4731 (1967).
17) K. Tachibana and K. Fukuda : Japan. J. Appl. Phys., **12** (1973) (in press).
18) B. van der Sijde : J. Quant. Spectr. Rad. Transfer, **12**, 703 (1972).
19) A. N. Chester : Phys. Rev., **169**, 184 (1968).
20) T. F. Johnston, Jr. : Appl. Phys. Letters, **17**, 161 (1970).
21) B. W. Shore and D. H. Menzel : *Principles of Atomic Spectra* (John Wiley and Sons, Inc., New York, 1968) p. 287.